Characteristic dielectric behaviour of the wide temperature range twist grain boundary phases of unsymmetrical liquid crystal dimers

2007 J. Phys.: Condens. Matter 19 436219

(http://iopscience.iop.org/0953-8984/19/43/436219)

IOP PUBLISHING JOURNAL OF PHYSICS: CONDENSED MATTER

J. Phys.: Condens. Matter **19** (2007) 436219 (12pp) doi:10.1088/0953-8984/19/43/436219

Characteristic dielectric behaviour of the wide temperature range twist grain boundary phases of unsymmetrical liquid crystal dimers

M B Pandey[1], R Dhar[1,2], A S Achalkumar[3] and C V Yelamaggad[3]

[1] Physics Department, University of Allahabad, Allahabad-211 002, India
[2] Physics Department, Ewing Christian College, Allahabad-211 003, India
[3] Centre for Liquid Crystal Research, Jalahalli, Bangalore-560 103, India

E-mail: dr_ravindra_dhar@hotmail.com

Received 16 July 2007, in final form 26 August 2007
Published 1 October 2007
Online at stacks.iop.org/JPhysCM/19/436219

Abstract

The investigated optically active dimeric compound, 4-*n*-undecyloxy-4′-(cholesteryloxycarbonyl-1-butyloxy)chalcone, shows wide temperature ranges of two twist grain boundary (TGB) phases, TGBA and TGBC*. Comprehensive dielectric studies have been carried out for this compound in the frequency range 1 Hz–10 MHz for different conditions of molecular anchoring. This compound shows negative dielectric anisotropy ($\Delta\varepsilon' = \varepsilon'_{\parallel} - \varepsilon'_{\perp} < 0$). Various electrical parameters, namely the dielectric permittivity, dielectric anisotropy, DC conductivity and activation energy, have been determined for these TGB phases. Weak relaxation processes have been detected in the TGBA and TGBC* phases, presumably due to amplitude (soft mode) and phase (Goldstone mode) fluctuations.

1. Introduction

Twist grain boundary (TGB) smectic A phase was first predicted in 1988 [1] and realized in 1989 [2] as a liquid crystal analogue of the type-II Abrikosov flux lattice. Over the past 18 years, many other TGB structures, namely TGBC, TGBC*, TGBC$^*_A$, TGBQ, etc, have been proposed, and most of them have been experimentally realized in pure systems as well as in mixtures [3–9]. In the TGBA, TGBC, and TGBC* phases, slabs of the molecules which have local smectic A (SmA), smectic C (SmC), and smectic C* (SmC*) structures respectively are rotated with respect to each other through an angle ($\Delta\psi$) by screw dislocations, resulting in the formation of a helical structure [1].

Dielectric studies of the TGB phases are scarce. So far, only a few reports in the literature are available on the dielectric behaviour of TGB phases [10–18]. This is because most TGB

phases exist over a very short temperature range due to their frustrated nature. Initial frequency-dependent (dynamic) dielectric studies of the TGBA phase [10–12] show that, like those of SmA* phase, an electric field induces amplitude fluctuation of the tilt angle, and hence a soft mode of dielectric relaxation is observed in the TGBA phase. Similarly, in the TGBC phase, an electric field induces phase fluctuation of the tilt angle, and hence a Goldstone mode of dielectric relaxation is observed like those in SmC* phase [13, 14]. However, experimental evidences suggest that TGB phase relaxation processes have lower amplitudes and higher relaxation frequencies as compared to those observed in the classical SmA* and SmC* phases. Ismaili *et al* [14] have proposed a theoretical model verified by some experimental work as well, which suggests that the Goldstone mode of the TGBC phase and the soft mode of the TGBA phase are strongly reduced due to the existence of an elastic parameter (H_2) in these phases. Ismaili *et al* have obtained the dielectric strength ($\delta\varepsilon_{\mathrm{G}}$) of the Goldstone mode of the TGBC phase and ($\delta\varepsilon_{\mathrm{S}}$) of the soft mode of the TGBA phase as [14]

$$\delta\varepsilon_{\mathrm{G}} = \frac{\varepsilon_0 \chi_e^2 C^2}{H_2} \cos\theta_{\mathrm{S}}^2 \tag{1}$$

and

$$\delta\varepsilon_{\mathrm{S}} = \frac{\varepsilon_0 \chi_e^2 C^2}{\alpha(T - T_{\mathrm{C}}) + H_2}, \tag{2}$$

with their respective relaxation frequencies as

$$f_{\mathrm{G}} = \frac{H_2}{2\pi\gamma_{\mathrm{G}}'} \tag{3}$$

and

$$f_{\mathrm{S}} = \frac{\alpha(T - T_{\mathrm{C}}) + H_2}{2\pi\gamma_{\mathrm{S}}}, \tag{4}$$

where

$$H_2 = \frac{8\beta_{\mathrm{a}}^2}{1 - \beta_{\mathrm{a}}^2/3} \frac{K_{22}}{l_{\mathrm{b}}^2}. \tag{5}$$

In equations (1)–(5), θ_{S} is the spontaneous tilt angle of the TGBC phase, C expresses the linear coupling between the tilt and the polarization, $T_{\mathrm{C}} = T_0 + \varepsilon_0 \chi_e C^2/\alpha$ with T_0 representing SmA–SmC transition temperature in a non-chiral compound. Existence of H_2 is connected to the elastic distortion of the director, and its amplitude depends strongly on the anchoring parameter (β_{a}) arising due to the anchoring forces at the grain boundaries and the distance between the grain boundaries (l_{b}). However, this theory has not been convincingly verified for general systems possessing various TGB phases. Above all, the problem of collective modes in the TGBC* phase is still an open question for both theoreticians and experimentalists. The aim of the present paper is to explore the expected modes of dielectric relaxations for wide temperature range TGB phases. There are very few systems showing TGB phases in a wide temperature range [16, 18]. Recently, exceptionally wide temperature range TGBA and TGBC* phases of unsymmetrical liquid crystal dimer, namely 4-*n*-undecyloxy-4′-(cholesteryloxycarbonyl-1-butyloxy)chalcone (molecular structure shown in figure 1) have been observed and reported [19]. We have chosen this system to carry out our investigations in order to obtain the dielectric behaviour of the stabilized TGB phases (especially that of the tilted TGB structure in the search for dielectric relaxation due to the phase fluctuation).

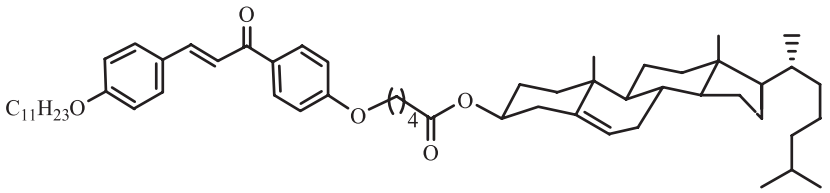

Figure 1. Molecular structure of a unsymmetrical liquid crystal dimer, namely 4-*n*-undecyloxy-4′-(cholesteryloxycarbonyl-1-butyloxy)chalcone.

2. Experimental details

The phase transition temperatures were determined by using a Perkin-Elmer differential scanning calorimeter and a transmitted light polarizing microscope. Dielectric studies of homeotropic and planar aligned samples were carried out by filling the samples in parallel plate capacitors made from indium tin oxide (ITO) coated glass plates (as electrodes) having sheet resistance less than 25 Ω. Depositing a thin layer of polyamide nylon on electrodes and then rubbing unidirectionally with soft cotton produces planar alignment (long axes parallel to the surface of the electrodes) of the molecules. For homeotropic alignment, the electrodes were coated with the lecithin. However, in the case of TGB phases, one should not expect that all the molecules will be orthogonal to the electrode surfaces like to those in nematic (N) and smectic A (SmA) phases. The active capacitance (C_A) of the cell was determined by using standard non-polar liquid (cyclohexane in the present case) as follows.

$$C_A = [C(\text{ch}) - C(\text{a})]/[\varepsilon'(\text{ch}) - 1], \tag{6}$$

where $C(\text{ch})$ and $C(\text{a})$ are the capacity of the capacitor with cyclohexane and air respectively inside the cell. $\varepsilon'(\text{ch})$ is the relative permittivity of the cyclohexane. Complete removal of the cyclohexane (after the calibration) from the cell was ensured by comparing the capacity of the cell before and after filling with cyclohexane.

Schematic diagrams of the arrangement of molecules in TGB phases in two measuring configurations are shown in figure 2. Two plates were separated by Mylar spacers of thickness 10 μm. Material was filled in the cell by capillary action at a temperature of about 10 °C above the transition to its isotropic liquid phase. Planar alignment of the molecules was spontaneously achieved while cooling the sample from its isotropic liquid phase to the TGBA phase. However, spontaneous homeotropic alignment (under cooling from the isotropic liquid to the TGBA phase) could not be possible. It could be possible only after shearing two glass electrodes with respect to each other in the TGBA phase. After getting almost perfect homeotropic alignment (with shear of the electrodes), the sample was further cooled to the lowest possible temperature in the TGBC* phase. However, we did not go to the very low temperature side of the TGBC* phase in order to avoid chance crystallization. Afterwards, the sample was again heated slowly to acquire data in the heating cycle. It is important to mention here that homeotropic alignment of TGB phases (specially TGBA) is quite difficult due to the competition between anchoring forces at the surfaces (to keep molecules normal to the bounding surfaces) and anchoring forces at grain boundaries, which tries to rotate the smectic blocks (which causes the molecules to deviate from being normal to the bounding surfaces). However, alignment improves in the tilted phases. A possible explanation of this will be given below, while discussing our results.

The capacitance and conductance of the cell filled with the sample were determined in the frequency range of 1 Hz–10 MHz using a Solartron impedance/gain-phase analyser (model SI-1260) coupled with a dielectric interface (model DI-1296). With the capacitance data, dielectric

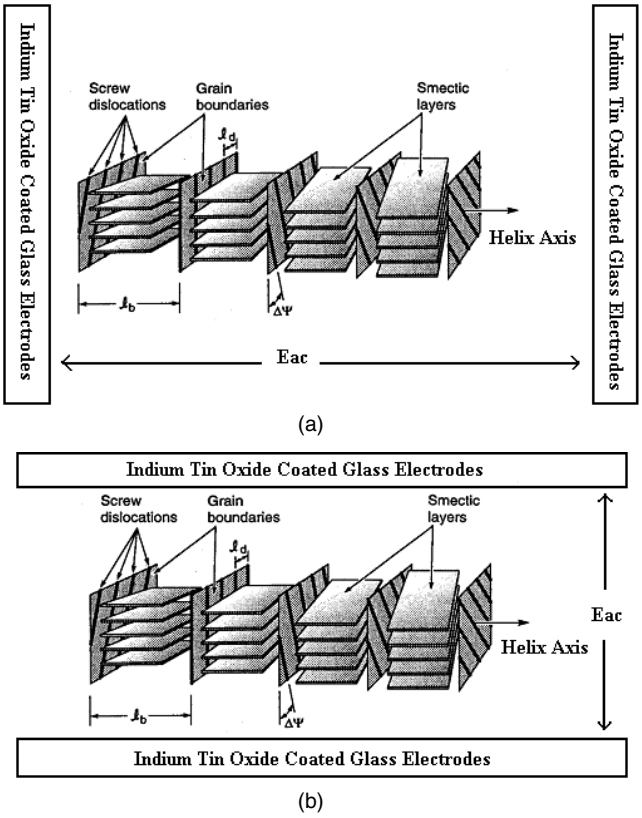

Figure 2. Schematic presentation of TGB phases (taken from [2]) confined between two electrodes under planar (a) and homeotropic (b) anchoring conditions of molecules.

permittivities in the homeotropic ($\varepsilon'_{\parallel}$) and planar ($\varepsilon'_{\perp}$) alignment of the molecules have been determined. Similarly, by using conductance data, conductivities in the homeotropic ($\sigma_{\parallel}$) and planar ($\sigma_{\perp}$) configurations have been obtained. The temperature of the sample for the electrical studies was controlled with the help of an Instec hot stage (model HS-1) with temperature accuracy of $\pm 0.1\,^{\circ}$C. The local temperature of the sample was verified by measuring the thermo emf of a copper–constantan thermocouple with the help of a six and a half digit multimeter. Other details of the experimental techniques have already been discussed elsewhere [20–23].

The instrumental uncertainties in the determinations of the transition temperatures and transition enthalpies (ΔH) with the help of differential scanning calorimetry (DSC) are $\pm 0.1\,^{\circ}$C and $\pm 2\%$ respectively. The accuracy in the measurement of capacitance (C) and conductance (G) in the concerned frequency range is $<0.2\%$, and hence the maximum uncertainty in the measurement of dielectric permittivity (ε') and conductivity (σ) within the entire frequency range is less than $\pm 1\%$. The accuracy of the measured frequency is ± 100 ppm.

3. Results and discussion

DSC thermograms in the heating and cooling cycles of the investigated compound at the scanning rate of $5\,^{\circ}$C min^{-1} are shown in figure 3. The investigated compound has the following phase sequences, as obtained by DSC and polarized light microscopic studies.

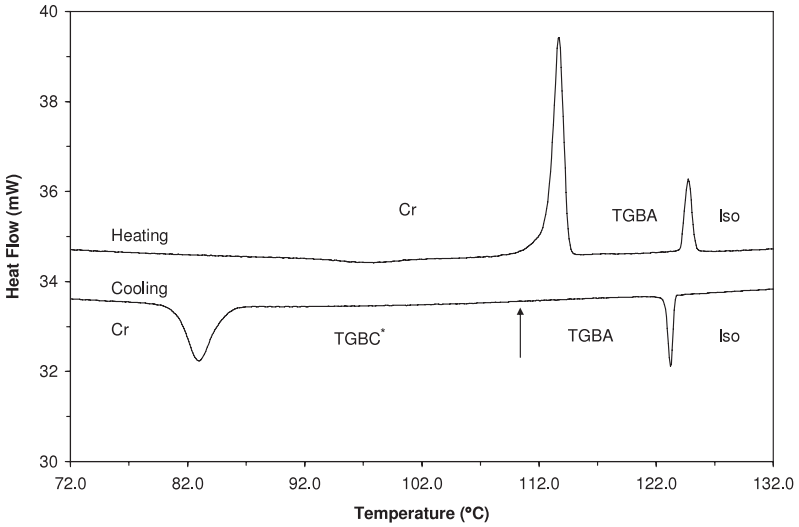

Figure 3. DSC thermogram at the scanning rate of 5 °C min^{-1} in the heating and cooling cycles.

Heating: Crystal 114.2 (41) TGBA 125.4 (7.8) Isotropic liquid

Cooling: Isotropic liquid 124.2 (7.7) TGBA 110.2 TGBC* 83.6 (24) Crystal

Data in the parentheses are enthalpies (J g^{-1}) whereas those outside the parentheses are transition temperatures (°C) associated with the phase transitions. The occurrence of a metastable TGBC* phase below the TGBA phase was adjudged based solely on the observation of characteristic optical textures. It showed undulated filaments or a square grid pattern when slides treated for the homeotropic or planar anchoring conditions were used, respectively. Typical optical textures of the homeotropic aligned sample are shown in figure 4.

3.1. Soft mode of the TGBA and TGBC phases*

The dielectric permittivity in the planar configuration ($\varepsilon'_\perp$) is almost constant in the frequency range 100 Hz–1 MHz for all the temperatures of the isotropic liquid phase, implying that no molecular relaxation exists in this phase. Data below 100 Hz and above 1 MHz are affected due to the electrode polarization capacitance and ITO effects, respectively [20, 21]. At the isotropic liquid to TGBA transition, $\varepsilon'_\perp$ increases very rapidly (see figure 5). On lowering the temperature in the TGBA phase below ∼119 °C, we observe that $\varepsilon'_\perp$ is no longer constant in the frequency range 100 Hz–1 MHz. $\varepsilon'_\perp$ shows some decrease for the frequencies above 100 kHz, indicating a pre-dielectric dispersion phenomenon in the frequency range 100 kHz–1 MHz (see figure 5). As the temperature goes down, this mechanism further dominates. From figure 5, one can see that, while going from 10 kHz to 1 MHz, $\varepsilon'_\perp$ decreases by ∼0.2 (at 111 °C). This indicates that the dielectric strength of the expected relaxation mode is very weak. Due to the weak dielectric strength and the dominance of the high-frequency correction term, we could not detect a peak of the dielectric loss curve, which is expected in the vicinity of 1 MHz. However, the dielectric strength increases upon lowering the temperature in the TGBA phase (see figure 5). In principle, one may expect soft mode relaxation in the TGBA phase under planar anchoring of the molecules [14, 16]. On the basis of the range of the relaxation frequency and its strength we speculate that this weak relaxation mode is a soft mode of the TGBA phase of the present material. It is important to mention here that the dielectric strength of the soft mode relaxation of the TGBA phase of some other molecular systems is of the same order [16].

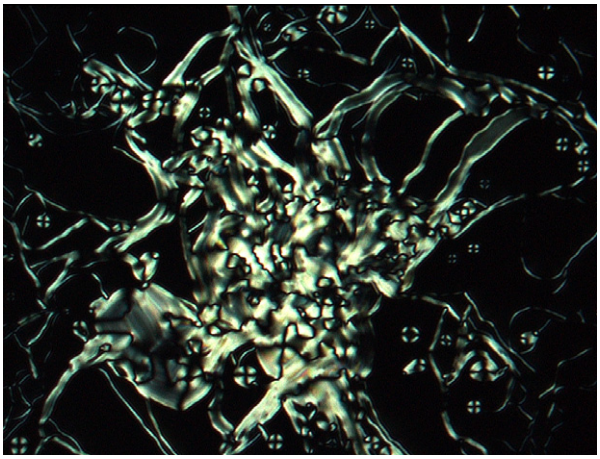

(a)

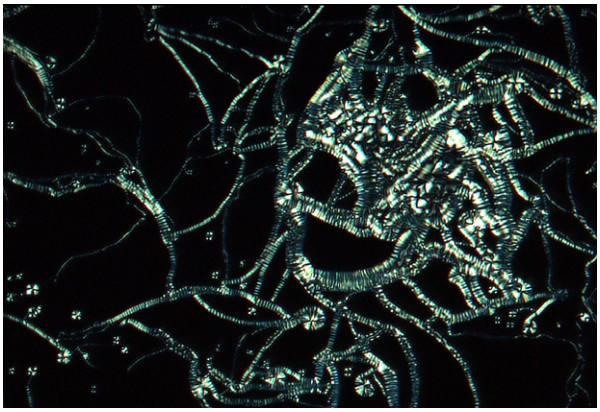

(b)

Figure 4. Typical optical textures of (a) TGBA phase at 122 °C and (b) TGBC* phase at 100 °C for the homeotropic aligned sample.

(This figure is in colour only in the electronic version)

At the TGBA–TGBC* transition, low-frequency values (10–100 Hz) of $\varepsilon'_\perp$ further increase; however, the high-frequency values of $\varepsilon'_\perp$ decrease (see figures 5 and 6). It is apparent from these dielectric data that the relaxation mode of the TGBA phase continues in the TGBC* phase as well, with increase in its strength. At the lowest temperature of the TGBC* phase, $\varepsilon'_\perp$ decreases from 4.8 to 4.4 while going from 10 kHz to 1 MHz. However, this strength is not yet sufficient to show a loss peak in the presence of the high-frequency parasitic effect at and around 1 MHz in the conductivity/loss data. From the dielectric data of the lowest temperature of the TGBC* phase, it is also clear that the relaxation frequency range of the observed mode (presumably the soft mode) of the TGBA/TGBC* phase is larger than that of the soft mode of the ferroelectric materials [22]. This is due to the presence of the elastic parameter H_2 (of TGB phases) in the numerator of equation (4). Similarly, the presence of H_2 in the denominator of equation (2) reduces the dielectric strengths of the soft mode of these TGB phases as compared to that of the SmA/SmC phases of the ferroelectric systems.

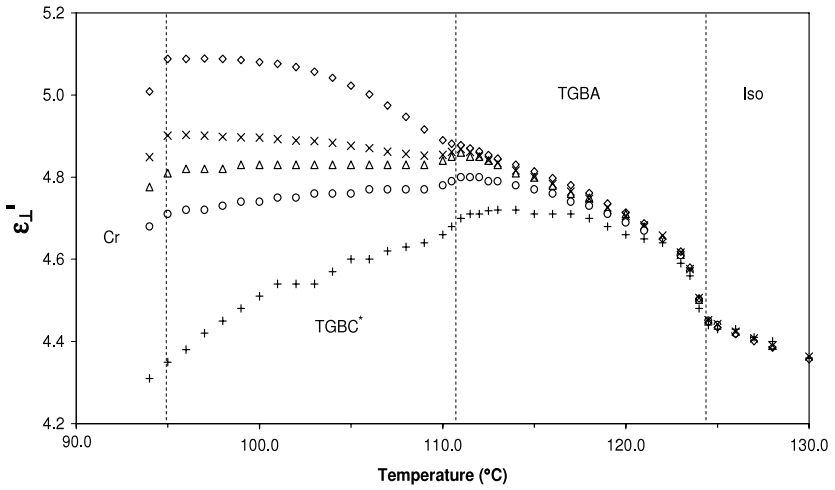

Figure 5. Variation of $\varepsilon'_{\perp}$ with temperature at 100 Hz (square), 1 kHz (cross), 10 kHz (triangle), 100 kHz (circle) and 1 MHz (plus). Broken vertical lines represent transition temperatures on the basis of the combined (thermodynamic, optical texture and dielectric) studies.

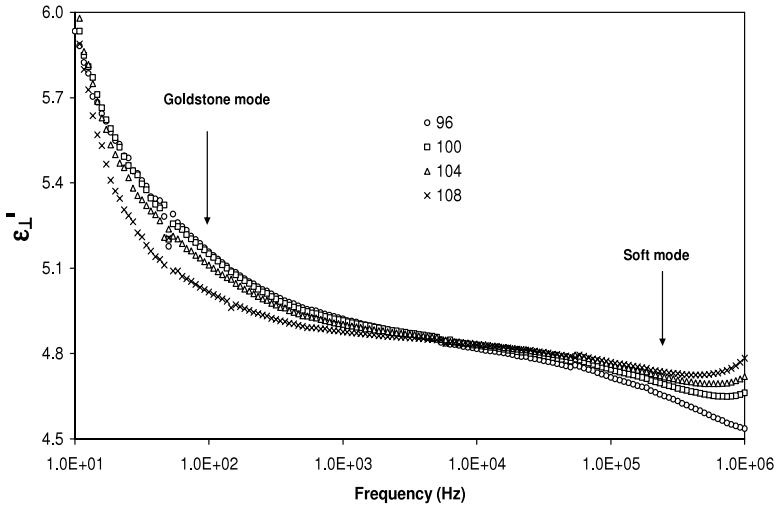

Figure 6. Variation of $\varepsilon'_{\perp}$ with frequency at 96, 100, 104 and 108 °C in the TGBC* phase to demonstrate signatures of the soft-like mode (on the higher-frequency side) and a Goldstone-like mode (on the lower-frequency side).

3.2. Goldstone mode of the TGBC phase*

In the low-frequency region (<1 kHz) of the TGBC* phase, $\varepsilon'_{\perp}$ increases upon decreasing the temperature. From figure 6, one can see that the value of $\varepsilon'_{\perp}$ increases upon cooling in the frequency range 1 kHz–10 Hz. This indicates the presence of another collective relaxation mechanism in this phase between 1 kHz and 10 Hz; however, data below 100 Hz are affected due to low-frequency parasitic contributions. It may be noted that low-frequency parasitic contributions will be more dominant at higher temperatures [23]. In the present case, the value of $\varepsilon'_{\perp}$ at 10 Hz is approximately the same at all temperatures of the TGBC* phase. Hence

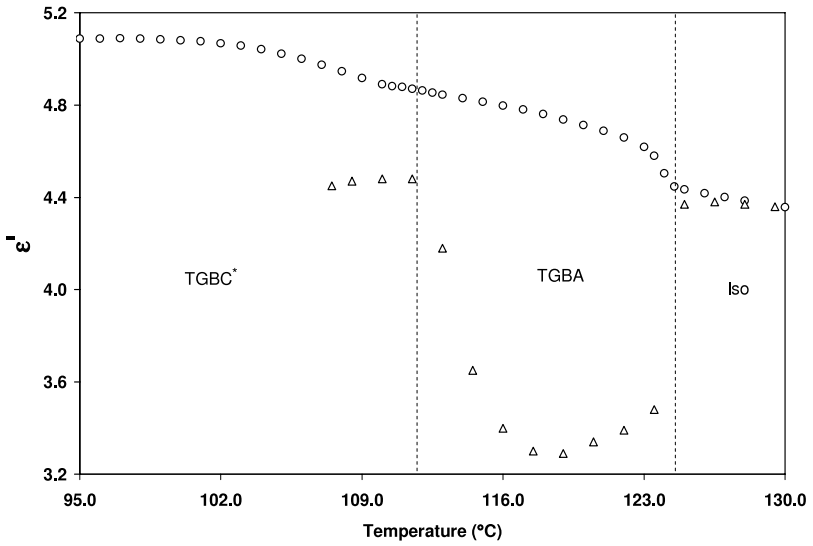

Figure 7. Variation of $\varepsilon'_{\parallel}$ (triangle) and $\varepsilon'_{\perp}$ (circle) with temperature at 100 Hz, indicating dielectric anisotropy ($\Delta\varepsilon'$) with the temperature. Broken vertical lines represent transition temperatures on the basis of the combined (thermodynamic, optical texture and dielectric) studies. The data for the planar aligned sample have been acquired during the cooling cycle whereas the data for the homeotropic aligned samples have been acquired during the heating cycle, as described in section 2. While acquiring data on the homeotropic aligned sample, we have not gone to the lower-temperature side of TGBC* phase in order to avoid chance crystallization.

the increase in the value of $\varepsilon'_{\perp}$ in the low-frequency region may be attributed to a relaxation mechanism. Since the relaxation frequency ($\sim$100 Hz) and dielectric strength of this mode remains constant (see figure 6) with temperature, we find that this mode is analogous to the Goldstone mode of the SmC* phase. Although theoretical modelling for the Goldstone mode of TGBC* is yet to be done, on the basis of the analogy of the TGBC phase one may conclude that low values of the relaxation frequencies (of the Goldstone-like mode of the TGBC* phase) may be due to the low value of the anchoring strength and high viscosity (see equation (3)) of the TGBC* phase of the present molecular system. The small value of the transverse component of the molecular dipole moment may be another reason for the weak Goldstone mode [23].

3.3. Dielectric anisotropy

Variations of $\varepsilon'_{\perp}$ and $\varepsilon'_{\parallel}$ (100 Hz) indicating variation of the dielectric anisotropy ($\Delta\varepsilon' = \varepsilon'_{\parallel} - \varepsilon'_{\perp}$) with the temperature are shown in figure 7. Keeping in mind that, in the case of homeotropic aligned TGB phases, all the molecules are not orthogonal to the electrode surfaces, it may be more illustrative to express the measured permittivity data in terms of the TGB helix axis. When we take the TGB helix axis as the reference axis then $\varepsilon'_{\perp}$ becomes $\varepsilon'_{\parallel \mathrm{h}}$, i.e. permittivity measured along the TGB helix axis (see figure 2(a)). Similarly, $\varepsilon'_{\parallel}$ becomes $\varepsilon'_{\perp \mathrm{h}}$, i.e. permittivity normal to the TGB helix axis (see figure 2(b)). As expected, in the isotropic liquid phase $\Delta\varepsilon'$ has been found to be $\widetilde{=}0$, showing that there is no preferred alignment of the molecules. Below the isotropic liquid to TGBA transition temperature ($T_{\mathrm{I-TGBA}}$), $\varepsilon'_{\perp}$ increases (whereas $\varepsilon'_{\parallel}$ decreases sharply) with decrease in the temperature, showing negative dielectric anisotropy ($\Delta\varepsilon' = \varepsilon'_{\parallel} - \varepsilon'_{\perp} < 0$) in the TGBA phase. Good planar alignment has not been achieved immediately below $T_{\mathrm{I-TGBA}}$, but as the temperature decreases in the TGBA phase, the molecular alignments

improve, and that is why $\varepsilon'_\perp$ increases quickly in the vicinity of the isotropic liquid to TGBA transition. After the perfect planar alignment, the rate of increase of $\varepsilon'_\perp$ becomes slow; however, an increasing trend continues throughout the TGBA phase. The dielectric anisotropy shows a minimum (~ -1.6) in the TGBA phase at about 118 °C. It is important to mention here that, in the case of the TGBA phase, planar oriented molecules are always orthogonal to the measuring electric field irrespective of the rotation of the smectic blocks (see figure 2(a)). Hence measurement of the transverse component of the permittivity ($\varepsilon'_\perp$) is usual (similar to that of the normal SmA phase). However, in the case of the cell treated for homeotropic alignment, the molecules are not always parallel to the measuring electric field due to rotation of the smectic blocks in the TGBA phase (see figure 2(b)). Hence it is expected that the measured value of the longitudinal component of the permittivity ($\varepsilon'_\parallel$) is lowered (as compared to virtual normal SmA phase of the same molecular system) due to the twisting of the smectic blocks in the TGBA phase. For this reason, values of $\varepsilon'_\parallel$ are unusually low in the TGBA phase (see figure 7). We say that this behaviour is unusual, because the average value of the measured dielectric permittivity ($\varepsilon'_{av} = (\varepsilon'_\parallel + 2\varepsilon'_\perp)/3$) for the TGBA phase is much lower than the extrapolated average value of the permittivity of the isotropic liquid phase for the TGBA phase.

A clear change in the slope of the $\varepsilon'_\perp$ data has been observed at $\sim$110 °C. This suggests a macroscopic change in the structure of the material at this temperature and confirms the existence of another phase below this temperature, which has also been observed during the polarized light microscopic study. As mentioned earlier, the observed square grid texture for the homogeneously (planar) aligned samples confirms this phase as TGBC* [19]. In the TGBC* phase, the 100 Hz data of $\varepsilon'_\perp$ are found to be invariant with temperature. However, the value of $\varepsilon'_\perp$ decreases slowly with decrease in temperature at higher frequencies, which is due to the dispersion phenomenon (of the Goldstone-like mode) around 200 Hz as discussed above. The presence of the Goldstone-like mode is also responsible for the increase in the 100 Hz data of $\varepsilon'_\perp$ at the TGBA–TGBC* transition. However, we again stress that the strength of the observed Goldstone-like mode is very weak in the present molecular system.

At the TGBA–TGBC* transition, $\varepsilon'_\parallel$ increases very rapidly by an appreciable magnitude. The increase in the value of $\varepsilon'_\parallel$ at the TGBA–TGBC* transition can be assigned to the tilt of molecules in the smectic blocks. Such a behaviour has also been observed in some other similar systems [17, 18]. In the TGBA phase, the molecules are always normal to the smectic layers. Hence with the rotation of smectic blocks and hence the layer planes (along the TGB helix), the molecules are also rotated and are no longer normal to the bounding surfaces (see figure 2(b) with SmA structure in the blocks). In the TGBC* phase, the rotating smectic blocks are filled with tilted helical SmC structure in such a way that the helix of the SmC* structure is always normal to the TGB helix. Hence it is just possible that the molecules of many more TGB blocks (as compared to the TGBA phase) are normal to the electrode surfaces (due to surface anchoring forces) whereas the blocks and hence the smectic layers are rotated by angle $\Delta\psi$. This causes an increase in the longitudinal component of the permittivity ($\varepsilon'_\parallel$) at the TGBA to TGBC* transition. This phenomenon also explains the better homeotropic alignment of the TGBC/C * structure as compared to TGBA by the bounding surfaces treatment technique. However, one should not ignore that TGBs in general, and the TGBC* structure in particular, are complex, and thus $\Delta\varepsilon'$ shown in figure 7 does not directly represent the dielectric anisotropy as defined for the simplest nematic and orthogonal smectics.

3.4. DC conductivity

The DC conductivity (σ(dc)) has been determined from the measured conductivity data in different phases of the investigated compound for planar and homeotropic alignments of the

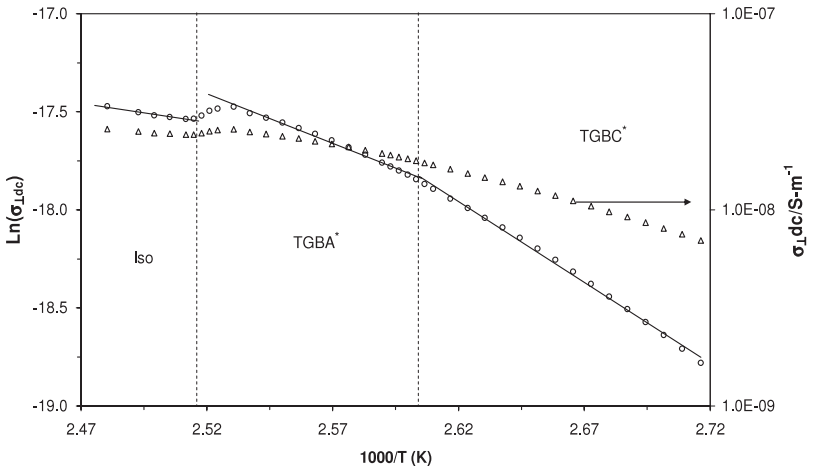

Figure 8. Variation of DC conductivity with temperature in various phases of the compound for the planar aligned sample. Broken vertical lines represent transition temperatures on the basis of the combined (thermodynamic, optical texture and dielectric) studies.

sample. For the planar oriented sample, it has been observed that the DC conductivity ($\sigma_\perp$(dc)) marginally increases at the isotropic liquid to TGBA transition (see figure 8). This gives confirmation that the TGBA phase has better ordering as compared to the isotropic liquid phase. In the case of planar oriented molecules of the TGBA and TGBC* phases, movement of ions is possible through interlayer spacings (see figure 2(a)). $\sigma_\perp$(dc) continuously decreases with decrease in the temperature throughout the TGBA and TGBC* phases, and follows an Arrhenius behaviour. This can be assigned to the increase in the viscosity of the material with decrease in temperature. The value of $\sigma_\perp$(dc) in the isotropic liquid and TGBA phases is of the order of 10^{-8} S m^{-1}, and it decreases to 10^{-9} S m^{-1} on the lower-temperature side of the TGBC* phase. No sharp change in the value of $\sigma_\perp$(dc) has been observed at the TGBA–TGBC* transition, but a change of slope distinguishes the two phases (see figure 8). The activation enthalpy of DC conductivity has been calculated in different phases using the following relation:

$$\sigma = \sigma_0 \exp\left(-\frac{E_A}{k_B T}\right), \tag{7}$$

where σ_0 is a constant, E_A is the activation enthalpy, T is the temperature in K and k_B ($=1.38 \times 10^{-23}$ J K^{-1}) is the Boltzman constant. Variation of ln (σ(dc)) with the inverse of absolute temperature ($1/T$) is shown in figure 8, which follows straight lines with different slopes in different phases. Activation enthalpies of the DC conductivity for different phases have been determined with the slopes of the straight lines obtained by the least-squares fit method. The values of activation enthalpies in the isotropic liquid, and TGBA and TGBC* phases are found to be 16, 42 and 69 kJ mol^{-1} respectively. The activation energy in the TGBC* phase is found to be approximately double that of the TGBA phase. It is supposed that the movements of the free ions are restricted upon lowering the temperature as well as due to tilting of the smectic blocks in the low-temperature TGBC* phase.

When the electrodes are treated for homeotropic anchoring (coated with the lecithin) it has been observed that σ(dc) increases by at least one order of magnitude even in the isotropic liquid phase. This has been the usual process in various types of material studied by us where lecithin has been used as surfactant. It seems that lecithin molecules contribute to the DC

conductance by injecting extra impurity ions, otherwise σ (dc) must be the same in both types of cell (planar and homeotropic) in the isotropic liquid phase of the samples as there must not be any preferred alignment of the molecules. For this reason, we are not reporting here results of the DC conductivity measured for homeotropic alignment of the molecules.

4. Conclusions

Thermodynamic, optical texture and dielectric studies unambiguously prove the occurrence of wide temperature range TGBA and TGBC* phases in the investigated compound. Weak transitions related with TGB phases have been clearly detected by the temperature dependence of the dielectric permittivity. The compound shows negative dielectric anisotropy. A weak relaxation process in the frequency range 100 kHz–1 MHz has been observed in both the TGB (A and C*) phases, presumably due to the soft mode behaviour. Another mode of relaxation has been detected in the TGBC* phase at around 200 Hz, and it has the signature of the Goldstone mode. In the present study we have succeeded in detecting these dielectric relaxation modes in the wide temperature range of TGBA and TGBC* phases. However, due to their weak dielectric strength, a quantitative analysis could not be carried out. Perhaps the synthesis of a molecular system with a large value of the transverse component of the dipole moment may yield independent clear characteristics of these modes.

Acknowledgments

We wish to thank the Department of Science and Technology (DST), New Delhi, for financial support under a project. The authors sincerely thank Professor H Prakash, Head, Physics Department, and Professor I M L Das, Physics Department, University of Allahabad, Allahabad, for their support.

References

[1] Renn S R and Lubensky T C 1988 *Phys. Rev.* A **38** 2132
[2] Goodby J W, Waugh M A, Stein S M, Chin E, Pindak R and Patel J S 1989 *Nature* **337** 449
Ihn K J, Zasadzinski J A N, Pindak R, Slaney A J and Goodby J W 1992 *Science* **258** 275
[3] Renn S R 1992 *Phys. Rev.* A **45** 953
[4] Kitzerow H S 2001 Twist grain boundary phases *Chirality in Liquid Crystals* ed H S Kitzerow and C Bahr (Berlin: Springer) pp 296–354 and references therein
[5] Petrenko A S, Hird M, Lewis R A, Meier J G, Jones J C and Goodby J W 2000 *J. Phys.: Condens. Matter* **12** 8577
[6] Lavrentovich O D, Nastishin Y A, Kulishov V I, Narkevich Y S and Tolochko A S 1990 *Europhys. Lett.* **13** 313
[7] Kuczynski W and Stegemeyer H 1995 *Mol. Cryst. Liq. Cryst.* **260** 377
[8] Dhar R, Pandey M B and Agrawal V K 2003 *Phase Transit.* **76** 763
[9] Dhar R, Pandey M B and Agrawal V K 2004 *Mol. Cryst. Liq. Cryst.* **409** 269
[10] Girold C, Legrand C, Isaert N, Pochat P, Parneix J P, Nguyen H T and Destrade C 1993 *Ferroelectrics* **147** 171
[11] Xu H, Panarin Y P, Vij J K, Seed A J, Hird M and Goodby J W 1995 *J. Phys.: Condens. Matter* **7** 7443
[12] Wrobel S, Hiller S, Pfeiffer M, Marzec M and Haase W 1995 *Liq. Cryst.* **18** 21
[13] Bougrioua F, Isaert N, Legrand C, Bouchta A, Barois P and Nguyen H T 1996 *Ferroelectrics* **180** 35
[14] Ismaili M, Bougrioua F, Isaert N, Legrand C and Nguyen H T 2001 *Phys. Rev.* E **65** 11701
[15] Srivastava S L and Dhar R 1998 *Mol. Cryst. Liq. Cryst.* **317** 23
[16] Gupta M, Dhar R, Agrawal V K, Dabrowski R and Tykarska M 2005 *Phys. Rev.* E **72** 021703
Dhar R 2006 *Phase Transit.* **79** 175
[17] Pandey M B 2004 Study of the chiral phases of liquid crystals *D. Phil Thesis* University of Allahabad, Allahabad, India

[18] Pandey M B, Dhar R and Kuczynski W 2006 *Ferroelectrics* **343** 69
[19] Yelamaggad C V, Achalkumar A S, Bonde N L and Prajapati A K 2006 *Chem. Mater.* **18** 1076
[20] Srivastava S L and Dhar R 1991 *Indian J. Pure Appl. Phys.* **29** 745
[21] Srivastava S L 1993 *Proc. Natl Acad. Sci. India* **63** 311
Dhar R 2004 *Indian J. Pure Appl. Phys.* **42** 56
[22] Pandey M B, Dhar R, Agrawal V K, Dabrowski R and Tykarska M 2004 *Liq. Cryst.* **31** 973
[23] Pandey M B, Dhar R, Agrawal V K, Khare R P and Dabrowski R 2003 *Phase Transit.* **76** 945